

# Heavy-Light Matrix Elements with the Wilson Quark Action\*

JLQCD Collaboration

S. Aoki<sup>a</sup>, M. Fukugita<sup>b</sup>, S. Hashimoto<sup>c</sup>, Y. Iwasaki<sup>a,d</sup>, K. Kanaya<sup>a,d</sup>, Y. Kuramashi<sup>c</sup>, H. Mino<sup>e</sup>,  
M. Okawa<sup>c</sup>, A. Ukawa<sup>a</sup>, T. Yoshié<sup>a,d</sup>

<sup>a</sup>Institute of Physics, University of Tsukuba, Tsukuba, Ibaraki 305, Japan

<sup>b</sup>Yukawa Institute for Theoretical Physics, Kyoto University, Kyoto 606, Japan

<sup>c</sup>National Laboratory for High Energy Physics (KEK), Tsukuba, Ibaraki 305, Japan

<sup>d</sup>Center for Computational Physics, University of Tsukuba, Tsukuba, Ibaraki 305, Japan

<sup>e</sup>Faculty of Engineering, Yamanashi University, Kofu 400, Japan

Status report is made of our quenched study of heavy-light matrix elements employing the Wilson quark action for heavy quark. Results obtained up to now with 200 configurations at  $\beta = 6.1$  on a  $24^3 \times 64$  lattice and with 100 configurations at  $\beta = 6.3$  on a  $32^3 \times 80$  lattice suggest that the pseudoscalar decay constant varies little over this range of  $\beta$  in both charm and bottom regions. Results for the  $B$  parameter are also reported.

## 1. Introduction

The  $B$  meson decay constant is an experimentally important quantity that can be calculated within the present techniques of lattice QCD. The calculations, however, would be hampered by a number of systematic effects and problems, which do not appear in the calculation for light quarks. We have been carrying out a set of quenched simulations covering the range of inverse lattice spacing  $a^{-1} = 2 - 4$  GeV employing the Wilson quark action to investigate systematic errors in the calculation. In particular, our prime aim is to see the effect of scaling violations in the decay constant associated with heavy quarks of  $O(m_Q a)$ , which allows various definitions of meson mass, and to examine whether the results continue to the static value at the infinite quark mass limit. In this article we report results obtained so far at  $\beta = 6.1$  and  $6.3$  using VPP500/80 at KEK.

## 2. Run Parameters and fitting procedure

In Table 1 we summarize parameters of our runs. The analyses reported in this article is

based on data sets, the statistics of which are doubled since the time of the Symposium.

We choose the spatial lattice size so that the physical lattice size is kept approximately constant at  $La \approx 1.9\text{fm}$ , which should be reasonably large to avoid finite-size effects for analyses of heavy-light meson properties. The temporal lattice size are taken large in order to ensure a reliable extraction of the ground state. Gauge configurations are generated with the 5-hit pseudoheatbath algorithm separated by 2000 sweeps for  $\beta = 6.1$  and 5000 for  $\beta = 6.3$ .

We take seven values of the heavy quark hopping parameter  $K_Q$  to cover the mass of charm and bottom quarks. Four values of light quark hopping parameter  $K_q$  are employed for an extrapolation to the chiral limit. In the heavy-light sector we calculate meson propagators for an arbitrary combination of  $K_q$  and  $K_Q$ . Light hadron propagators are evaluated only for the degenerate case.

Quark propagators are obtained with the red/black minimal residual algorithm for the point and wall sources in the Coulomb gauge, and local operators are used for sink.

For  $\chi^2$  fitting of hadron propagators we employ

\*Presented by S. Hashimoto

Table 1  
Parameters of runs.

$\beta$	6.1	6.3
size	$24^3 \times 64$	$32^3 \times 80$
$K_q$	0.1520 – 0.1543	0.1500 – 0.1513
$K_Q$	0.070 – 0.142	0.086 – 0.140
#conf.	200	100
$L$ (fm)	1.88(7)	1.89(8)
$a^{-1}$ (GeV)	2.56(9)	3.38(15)
$f_\pi$ (MeV)	122(3)	131(4)
$\Lambda_{\overline{MS}}^{(0)}$ (MeV)	239(8)	246(11)
$K_c$	0.15499(1)	0.15183(1)
$K_{strange}$	0.1531(1)	0.1505(1)

a single exponential uncorrelated fit with a single elimination jackknife analysis to estimate errors of masses and amplitudes. For the fitting interval  $[t_{min}, t_{max}]$ , we take [14,26] at  $\beta=6.1$  and [16,32] at  $\beta = 6.3$ . These are chosen by the conditions that the point and wall source results for effective mass overlap at  $t_{min}$ , and that  $t_{max}$  should be as large as possible until errors become unacceptably large and the fit becomes unstable.

### 3. Scale setting

We employ the  $\rho$  meson mass extrapolated to the chiral limit to fix the physical scale of lattice spacing. Results obtained with the wall source are listed in Table 1 together with the critical hopping parameter  $K_c$  and the value of  $K$  corresponding to the strange quark determined from  $m_K/m_\rho$ . Values for the point source are consistent, albeit with an error of order 50% larger for  $a^{-1}$ . The lattice spacing at  $\beta = 6.1$  is consistent with previous estimates in the range  $\beta \approx 6.0 - 6.2$ [1], while that at  $\beta = 6.3$  is 10% higher than the value reported in Ref. [2].

We also list in Table 1 our results for the pion decay constant  $f_\pi$  using the physical scale as estimated above. For the renormalization factor we employ the tadpole improved one-loop result[3]  $Z_A = (1 - 0.31\alpha_V(1/a))/8K_c$  which equals 0.750 at  $\beta=6.1$  and 0.772 at  $\beta=6.3$ . We observe that the value of  $f_\pi$  is two standard deviations smaller than the physical value at  $\beta=6.1$  in contrast with the case of  $\beta=6.3$  where they are consistent.

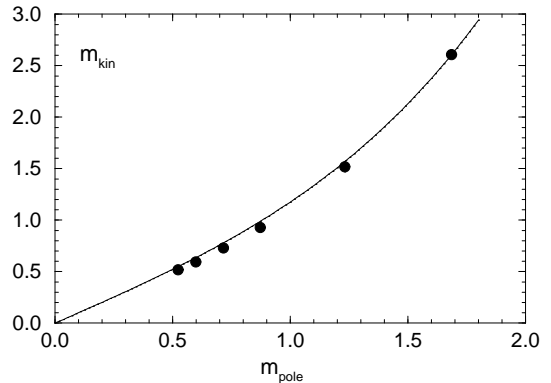


Figure 1. Kinetic mass as a function of pole mass at  $\beta = 6.3$  for heavy-light meson. Light quark mass is fixed at  $K_q = 0.1505$ . Solid curve represents the relation  $m_{kin} = \sinh m_{pole}$ .

Finally the QCD  $\Lambda$  parameter  $\Lambda_{\overline{MS}}^{(0)}$  estimated from the tadpole-improved  $\overline{MS}$  coupling constant indicates the presence of a small violation of asymptotic scaling in this quantity, as has been known from previous work[1].

### 4. Heavy meson kinetic mass

A manifestation of  $O(m_Q a)$  effects for the Wilson quark action appears in the discrepancy of the pole mass  $m_{pole}$  and the kinetic mass  $m_{kin}$  defined by an expansion of energy of the form,

$$E = m_{pole} + \frac{\hat{p}^2}{2m_{kin}} - c \frac{\hat{p}^4}{8m_{kin}^3} + \dots \quad (1)$$

where  $\hat{p}^2 = \sum_{i=1}^3 (2 \sin p_i / 2)^2$  and the constant  $c$  parametrizes relativistic corrections. It has been argued[4] that dynamical scales of heavy-light mesons are controlled by the kinetic mass, and hence it is a physically more relevant mass parameter than the pole mass. We adopt this view and examine the mass dependence of the decay constant in terms of the kinetic mass.

In Fig. 1 we illustrate our data for the two masses. The kinetic mass is extracted by a fit of the measured dispersion relation using four values of momenta up to (1, 1, 1) in terms of (1). It is interesting to observe that the relation of the two masses are reasonably described by the form  $m_{kin} = \sinh m_{pole}$  which follows from the disper-

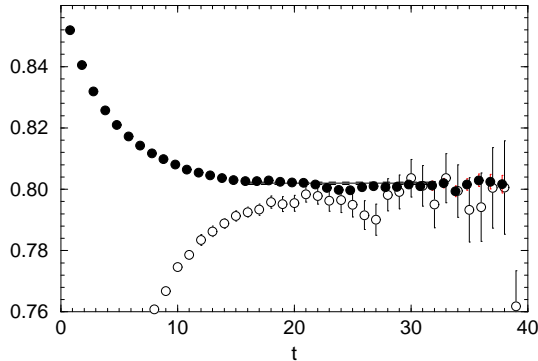


Figure 2. Ratio of correlation functions in (3) for point (open circles) and wall (filled circles) source for  $K_Q=0.086$  and  $K_q=0.1505$  at  $\beta=6.3$ . Solid and dashed lines are fit value and error as explained in text.

sion relation for a free scalar particle given by  $(2 \sinh(\frac{E}{2}))^2 = m_0^2 + \hat{p}^2$ [5]. The relation, however, is not accurate in the region of charmed meson.

### 5. Heavy-light decay constant

Our method to obtain the lattice value of the heavy-light decay constant is summarized by

$$(f_P \sqrt{m_P})^{lat} = \sqrt{8K_c - 6K_q} \sqrt{8K_c - 6K_Q} \times Z^{A/P} \sqrt{2Z^P}. \quad (2)$$

The first two factors represent the non-relativistic normalization for the quark wave function[4,6]. The constant  $Z^{A/P}$  is extracted from the relation,

$$\frac{\langle 0 | A_4(t) P(0)_s^\dagger | 0 \rangle}{\langle 0 | P(t) P(0)_s^\dagger | 0 \rangle} \xrightarrow{t \gg 1} Z^{A/P} \tanh m_{\text{pole}}(t - L_t/2). \quad (3)$$

Here  $A_4$  and  $P$  at time  $t$  are the local axial-vector and pseudoscalar currents, the subscript  $s$  at time  $t = 0$  denotes the type of source, and the hyperbolic tangent takes into account the change of sign of the numerator at half the temporal lattice size  $L_t/2$ . The amplitude  $Z^P$  is defined in terms of the point-to-point pseudoscalar propagator through

$$\langle 0 | P(t) P(0)_s^\dagger | 0 \rangle \xrightarrow{t \gg 1} 2Z^P \cosh m_{\text{pole}}(t - L_t/2). \quad (4)$$

In Fig. 2 we plot a typical example of the ratio of propagators in (3). Data for the ratio for the

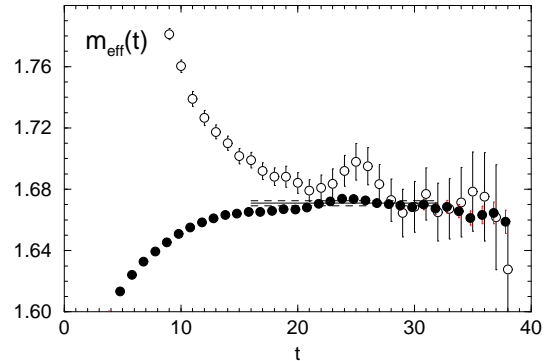


Figure 3. Effective mass for heavy-light meson. Parameters and meaning of symbols are the same as in Fig. 2.

wall source exhibits a smooth behavior with small errors of 1% or less for any value of the hopping parameter we took. Thus the constant  $Z^{A/P}$  can be reliably determined.

For an extraction of the amplitude  $Z^P$  we employed a single hyperbolic cosine fit to the point-to-point pseudoscalar propagator at the time of the Symposium. We observed that this is problematical when the heavy quark hopping parameter becomes small because of a rapid increase of fluctuations. This is illustrated in Fig. 3 which shows the effective mass of the heavy-light meson at our smallest value of  $K_Q$ : no clear signal of plateau can be seen for the point-to-point propagator (open circles).

An alternative procedure, facilitated by the fact that signals are much better for the wall source, is to apply a simultaneous fit to the point-to-point and point-to-wall propagators assuming a common mass. We find that the fit becomes much more stable and that the fitted value of  $Z^P$  over subsets of configurations fluctuates much less. We therefore adopt this procedure to extract the value of  $Z^P$ . An example of the fitted value and the error for mass is shown in Fig. 3 (solid and dashed lines).

At  $\beta = 6.3$  we may compare our results for lattice value of  $f_P \sqrt{m_P}$  with those of Ref. [7]. Applying the same analysis procedure as ours to their data we find that the two sets of results are consistent within the error.

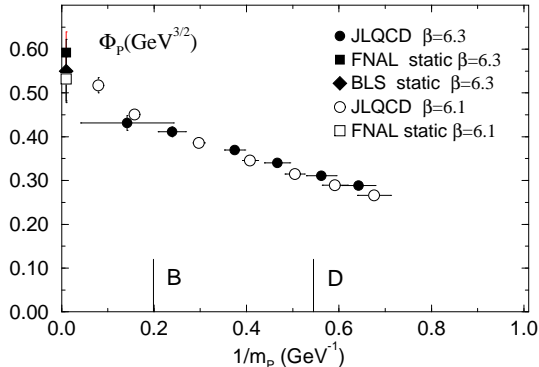


Figure 4.  $\Phi_P$  as a function of inverse kinetic mass  $1/m_P$  in physical units.

We employ the tadpole-improved one-loop renormalization factor  $Z_A$ , already encountered for  $f_\pi$ , to convert lattice results for  $f_P\sqrt{m_P}$  to those in the continuum. Since this factor refers to the case of zero quark mass, an uncertainty of  $O(\alpha_s m_Q a)$  remains in our final result. In Fig. 4 we plot the scale invariant quantity

$$\Phi_P = \left( \frac{\alpha_s(m_P)}{\alpha_s(m_B)} \right)^{2/\beta_0} f_P \sqrt{m_P} \quad (5)$$

as a function of the inverse of meson mass  $1/m_P$  for both  $\beta=6.1$  and  $6.3$ , where we take the measured kinetic mass for  $m_P$ . We also plot the static values taken from Refs. [2,7] for comparison. Conversion to physical units is made with the lattice spacing listed in Table 1.

We observe that the results at the two values of  $\beta$  agree with each other, and they seem to continue smoothly to the static value. Errors in the kinetic mass and statistical fluctuations arising from point-to-point propagators in the values for  $\Phi_P$ , however, are still large to tell conclusively whether large  $O(m_Q a)$  effects are absent for the heavy-light meson decay constant. We remark that this result is obtained when  $\Phi_P$  is plotted with respect to the measured kinetic mass.

We fit results for  $\Phi_P$  to a quadratic form  $\Phi_P = c_0(1 + c_1/m_P + c_2/m_P^2)$  to obtain the values at the physical  $B$  and  $D$  mesons. Our results for  $f_B$ ,  $f_{B_s}$ ,  $f_D$  and  $f_{D_s}$  are given in Table 2. Statistical errors include uncertainties in the kinetic mass to the extent that a jackknife analysis eliminating

Table 2

Decay constant and  $B$  parameter for  $B$  and  $D$  mesons. First error is statistical and second that of scale determined from  $m_\rho$ .

$\beta$	6.1	6.3
$f_B$ (MeV)	192(5)(10)	182(10)(12)
$f_{B_s}$ (MeV)	228(4)(12)	215(4)(14)
$f_{B_s}/f_B$	1.19(3)	1.18(6)
$f_D$ (MeV)	206(5)(11)	216(9)(14)
$f_{D_s}$ (MeV)	237(4)(13)	240(4)(16)
$f_{D_s}/f_D$	1.16(3)	1.11(5)
$B_B$	0.895(47)	0.840(60)
$B_{B_s}$	0.889(24)	0.878(32)

single gauge configuration at a time is applied to the fitting of  $\Phi_P$ .

## 6. $B$ meson $B$ parameter

We also calculate the  $B$  meson  $B$  parameter from a ratio of three- and two-point functions and the  $\Delta B = 2$  weak operator fixed at the origin of lattice. One-loop renormalization factors evaluated with the tadpole-improved coupling  $\alpha_V(1/a)$  are used for relating the lattice value to that in the continuum. Our results for  $B_B$  and  $B_{B_s}$  at  $\mu=5\text{GeV}$  are tabulated in Table 2, which are consistent with results reported previously[8,9].

## REFERENCES

1. For a review, see, *e.g.*, A. Ukawa, Nucl. Phys. B(Proc. Suppl.) 30 (1993) 3.
2. A. Duncan *et al.*, Phys. Rev. D51 (1995) 5101.
3. G.P. Lepage and P. Mackenzie, Phys. Rev. D48 (1993) 2250.
4. See, *e.g.*, G. P. Lepage, Nucl. Phys. B (Proc. Suppl.) 26 (1992) 45.
5. T. Bhattacharya and R. Gupta, Nucl. Phys. B (Proc. Suppl.) 42 (1995) 935.
6. A. Kronfeld, Nucl. Phys. B(Proc. Suppl.) 34 (1994) 415 and references cited therein.
7. C. Bernard, J. Labrenz and A. Soni, Phys. Rev. D49 (1994) 2536.
8. C. Bernard *et al.*, Phys. Rev. D38 (1988) 3540.
9. A. Abada *et al.*, Nucl. Phys. B376 (1992) 172.